ORIGINAL PAPER

A statistical approach to investigate the effects of multicomponent fractions on the mechanical properties of PP/PPMA/Talc/POE composites

Mojtaba Ajorloo[1] · Maryam Ghodrat[2,3] · Mohammad Reza Moghbeli[4] · Won-Hee Kang[3]

Abstract
An immense technological challenge of polypropylene-based composites is in optimising the effect of multicomponent fractions on their mechanical properties. Hence the main aim of the present study is to carry out a systematic statistical approach to investigate the impact of multicomponent fractions on the mechanical properties of Polypropylene (PP)/Talc/ Polyolefin Elastomer (POE) and maleic-anhydride-grafted Polypropylene (PPMA) composites. Response Surface Methodology (RSM) based on Central Composite Design (CCD) has been implemented as the design of experiment technique. With respect to CCD and three different weight percentages of Talc (0, 15, 30 wt%), POE (0, 10, 20 wt%), and PPMA (0, 2.5, 5 wt%), 17 experiments were designed and prepared via a conventional melt blending technique. Analysis of variance (ANOVA) with diagnostic figures has been proposed to derive mathematical models to predict the mechanical properties of the utilised PP based composite. The findings showed that the concentration of POE, particularly at a lower amount, play a significant role and can predominantly affect the properties of the composites. The results also revealed that in spite of Talc and PPMA, adding of POE caused a noticeable rise in ductility and toughness of composite and a reduction in the stiffness. It was also found that all the assessed properties can be maximized simultaneously, providing the content of Talc, POE, and PPMA set to be 30%, 6.228%, and 2.514%, respectively. The findings are found to be aligned with the scanning electron microscopy micrographs and the DSC analysis data.

Keywords Polypropylene · Mechanical properties · Design of Experiment · RSM · Auto interior and exterior parts · Talc-POE · Coupling agent

Introduction

Due to the outstanding properties such as excellent chemical resistance, low density, reasonable price, good process-ability and acceptable stress crack resistance, polypropylene (PP) is known as a multipurpose product and one of the most widely used commodities in many industries for automobile, construction, pipeline, and packaging [1–6]. However, poor impact fracture, especially, at a low temperature, is the most significant shortcoming that restricts PP when used as an engineering material [7–10]. This issue is the main reason for further research in this field. Based on the fact that rubbery materials have good impact toughness, blending PP with a rubbery substance is a practical method to boost the impact strength [11–13]. In comparison to conventional impact modifiers such as Ethylene-Propylene Rubber (EPR) and Ethylene-Propylene Diene Monomers (EPDM), the efficiency of Polyolefin Elastomer (POE), POE-toughed, systems are fairly higher. The main reason is due to their acceptable compatibility with PP along with an easier process-ability [2, 14, 15]. The results of the study conducted by Tang et al. [13] depicted a considerable increase in the impact strength of PP with 10% of POE because of more straightforward cavitation and shear yielding of the matrix. However, Liang [16] reported that the incorporation of POE reduces the flexural and

✉ Maryam Ghodrat
m.ghodrat@adfa.edu.au

1 School of Chemical, Petroleum and Gas Engineering, Iran University of Science and Technology, 16846-13114 Tehran, Iran

2 School of Engineering and Information Technology, The University of New South Wales , Canberra, ACT 2600, Australia

3 Centre for Infrastructure Engineering, Western Sydney University, Penrith, NSW 2751, Australia

4 Department of Chemical engineering, Iran University of science and Technology, Tehran, Iran

tensile moduli and the strength, considerably. Therefore, using elastomers leads to an improvement in toughness, while it deteriorates the stiffness of the composite [12, 17, 18].

Fillers, which were adopted initially as a cost-reducing agent, are now considered in a reinforcing phase in polymeric composites [19, 20]. In many studies in the literature, the impacts of mineral fillers on the properties of PP-based composites have been investigated [21–26]. These studies showed that applications of inorganic fillers lead to the improvement in stiffness, hardness and dimensional stability. Among all types of mineral fillers, Talc, which is composed of hydrated magnesium silicate with chemical formula $Mg_3Si_4O_{10}(OH)_2$, is the most prevalent and widely used filler to enhance the properties of PP and to reduce the cost [3, 27, 28]. Moreover, the role of Talc as a nucleating agent and its influences on the crystallization behaviour and morphology of PP chains have been reported repeatedly [19, 29, 30].

Owing to the non-polar and hydrophobic nature of polyolefins, their interaction with inorganic fillers, which are hydrophilic intrinsically, is a challenging matter [3, 18, 21], so that the uniform dispersion and distribution of filler particulates in a polymeric matrix cannot be achieved easily. Besides, under this circumstance, the interfacial adhesion is not formed flawlessly, and the applied stress cannot be transferred from the matrix to the reinforcing phase efficiently [21, 27]. The utilization of an appropriate compatibilizer such as maleic-anhydride-grafted Polypropylene (PPMA) has been introduced as a practical method to obtain a high performance filler-reinforced polymeric composites in many articles [31, 32]. The reaction between active groups on the surface of filler and the maleic anhydride from coupling agent causes convincing filler dispersion and enhances the matrix/filler interactions. Jahani [3] studied the properties of chemically coupled Talc-filled PP composites and revealed that the PPMA coupling agent affected the mechanical properties, particularly the tensile strength, significantly. More recently, PP/Elastomer/Filler ternary composites have become more popular in applications that both toughness and stiffness are dominant influential parameters. Wu et al. [11] studied the properties of PP/Talc/POE ternary composites and showed the enhancement in the toughness of the samples compared to the neat blends. They also found no remarkable reduction in stiffness and tensile strength.

However, none of the previous studies identified the specific impact of each parameter and also the interaction between them on the mechanical properties of PP/Talc/POE/PPMA composites, which is not achievable through conventional experimental methods. To the best of the authors' knowledge, this is the first study which investigates the properties of the abovementioned composites from the statistical point of view. The main purpose of this work, therefore, is to present a new approach to determine not only the effect of each parameter but also the interactions on the mechanical

properties of Talc-filled and POE-toughened composites. This study also aims to develop quantitative prediction models for the mechanical properties of PP/Talc/POE/PPMA composites employing response surface methodology (RSM). The optimized formulation of PP/Talc/POE/PPMA can be designed for different applications with the aid of the first-time proposed prediction models in various industries, in particular, the automotive industry. This technique is an effective approach, which helps to avoid costly and time-consuming experimental tests. RSM statistically identifies the correlations between several independent variables and one or more responses [33]. This method also gives an insight into the impacts of each variable on the foremost mechanical properties affecting the performance of automobile interior parts [1, 34].

Experimental

Material

The Polypropylene used in this work was a commercial-grade (Jampilen EP 440 L) with melt flow index (MFI) of 6.0 $g/10\ min$ (ASTM D1238 at 230 °C /2.16 kg), supplied by a local manufacturer, Jam Petrochemical Co. in Iran. The maleic-anhydride-grafted polypropylene (PPMA) with the trade name Aria Couple 1405 and with MFI 10 $g/10\ min$ (ASTM D1238 at 230 °C/2.16 kg) and the density of 0.96 g/cm^3 was provided from Aria Polymer Pishgam Co. in Iran, and it was used as the adhesion promoter. The employed POE (Solumer 875 L) was an ethylene-octene copolymer grade from SK Global Chemical Co. in Korea with MFI (ASTM D1238 at 190 °C/2.16 kg) of 5 $g/10\ min$. The Talc (Talc A1) with a mean particle size of 5 μm was supplied by Omya Pars Co. in Iran.

Sample preparation

To get compounds prepared, Coperion Werner Pfleiderer ZSK-25 WLE co-rotating twin-screw extruder, with L/D = 40 and the screw diameter of 25 mm, was utilized. Two loss-in-weight feeders were employed to convey raw materials to the extruder. The side feeder was dedicated to filler, and other pellet-form materials according to recipes were fed into the hopper through the main feeder. The speed of screw was set on 600 rpm, and the feeding rate was 30 kg/h. The temperature of different zones of the barrel from hopper to die was set, as shown in Table 1. To prepare tensile and Izod impact test specimens, an injection-molding machine, manufactured by

Table 1 Temperature Profile from Hopper to Die Head

Zone No.	1	2	3	4	5	6	7	8	9	10
Temp (°C)	195	205	210	215	205	200	195	195	205	210

Poolad Co. in Iran, was employed. The hopper to nozzle temperature was ranged from 180 to 210 °C.

Characterization

According to the ASTM D638 test method, to determine the tensile properties, a Zwick/Roell Machine (model z100) at a crosshead speed of 50 *mm/min* was implemented. The impact properties of the samples were measured according to ASTM D256A by a Zwick/Roell B5102 pendulum impact tester. The melt flow rate measurement was conducted according to ASTM D1238 by Ceast Junior Melt Flow Index tester at 230 °C.

To pinpoint the role of filler, impact modifier, and compatibilizer in changing mechanical properties of the prepared composites, experimental analyses were carried out, and the findings were compared with the modeling results. For this purpose, the benefit of filler dispersion, filler-matrix interactions, morphology of the dispersed POE phase through the matrix, plus the crystallinity of the samples, were investigated by scanning electron microscopy (SEM) images and differential scanning calorimetry (DSC) analysis. These tests can fundamentally regulate the properties of the filled and toughened composites.

The SEM images taken from the fractured surface of the Izod impact test specimens were employed to assess the microstructure and morphology of the samples. SEM images were obtained with the contribution of VEGA-LL TESCAN apparatus. Samples containing dispersed droplets of POE were etched in toluene at 50 °C for 12 h. To avoid an accumulation of electrical charges during the test, the surfaces of the specimens were sputtered with a thin layer of gold.

The DSC analysis was utilized to evaluate the thermal characteristic of the samples. The DSC analysis was performed with an apparatus manufactured by Sanaf Co. in Iran. The samples first were heated from ambient temperature to 200 °C with the rate of 10 °C/min. To erase the thermal history, the samples were kept at 200 °C for 5 *min*, after which a crystallization and cooling steps took place with the same rate and thermal scope. The necessary data were gathered from the second heating process performed with the same conditions. Data obtained from the cooling and heating curves were used to extract the melting temperature, crystallization temperature and degree of crystallinity of each sample.

Design of Experiments

In the present work, using the contribution of Design-Expert® 11 software, RSM with the Face-Centered ($\alpha =$ 1) Central Composite design (CCD) was employed. CCD is the most prevalent design for estimating the coefficients

of a quadratic regression [35]. Unlike Box-Behnken design (BBD), which lacks factorial points, CCD is notably helpful in sequential experiments because the information of previous factorial experiments can often be employed for a new design by adding new axial and center points. Besides, CCD considers points where all factors are simultaneously at their −1 or + 1 surface. According to Table 2, three independent variables (Talc, POE, and PPMA) with three surfaces for each of them (−1, 0, and 1) were determined.

In conformity with the number of variables and surfaces, a total of 17 experimental runs, presented in Table 3, were suggested by the software. It should be noted that the total number of experiments in CCD can be obtained from Eq. (1).

$$N = 2^k + (2 \times k) + C \tag{1}$$

Where N is the total number of design points, k is the number of variables and C is the number of central points. From those 17 experiments, 2^3 were factorial points, 2×3 were axial points, and 3 runs were dedicated to the central point to check the reproducibility of the samples.

Results and discussions

In this section, first, analysis of variance (ANOVA) is employed to derive significant models and to investigate the impact of the variables, i.e., Talc, POE, PPMA, and also their interactions on the mechanical properties (elastic modulus, tensile strength, elongation at break and impact strength) as responses of the design. An ANOVA test is a practical way to find out whether the results of a survey or experiment are significant. In other words, it helps to figure out if the null hypothesis needs to be rejected or the alternate hypothesis needs to be accepted [36, 37]. Second, with the contribution of RSM optimization tools, an optimized formulation meeting the requirements of a specific application is obtained. Finally, by comparing experimental and predicted values and adopting SEM micrographs and DSC data, the validity of modeling is evaluated through this section.

Table 2 Variables in CCD Design

Parameter	Name	Unit	−1	0	1
A	Talc	%	0	15	30
B	POE	%	0	10	20
C	PPMA	%	0	2.5	5

Table 3   Suggested Experiments

Variables	Run																
	1	2	3	4	5	6	7	8	9	10	11	12	13	14	15	16	17
Talc%	0	0	0	0	0	15	15	15	15	15	15	15	30	30	30	30	30
POE%	0	0	10	20	20	10	10	10	0	10	20	10	20	20	0	10	0
PPMA%	5	0	2.5	5	0	0	2.5	5	2.5	2.5	2.5	2.5	0	5	0	2.5	5

Mechanical properties-responses

Elastic Modulus

The ANOVA analysis of the quadratic model of elastic modulus is presented in Table 4. For a 95% confidence level, one factor is usually considered significant when the p value is less than 0.05 [38]. As can be seen, the p value of the model is smaller than 0.05, so that the model is significant. Besides, not significant lack-of-fit indicates the reliability of the model. Lack-of-fit is the amount that the model predictions miss the observations. Significant lack-of-fit indicates that the model does not fit the data within the observed replicate variation. R-squared indicates how well the model fits experimental data, and R-squared closer to 100% shows a more validity of the model. In this study, R-squared and lack-of-fit were two factors contributed to finding out a quadratic model as an appropriate one predicting the properties of PP/Talc/POE ternary composites containing PPMA coupling agent.

Eq. (2) represents the general function of the second-order polynomial regression used by RSM [39].

$$Y = \beta_0 + \sum_{i=1}^{k}\beta_i X_i + \sum_{i=1}^{k}\beta_{ii}X_i^2 + \sum\sum_{i<j=2}^{k}\beta_{ij}X_iX_j \quad (2)$$

where X_i and Y are variables and the answer, respectively, the term ε shows the error of the prediction, β_0 is a constant, β_i is the coefficient of the main effects of the variables, β_{ii} is the quadratic coefficient of variables, and β_{ij} is the coefficient of variables' interactions.

Based on ANOVA analysis, the model predicting the elastic modulus (E) of the composite is presented as Eq. (3). The presented equation is in the form of coded factors as follows:

$$E = 1440.54 + 266.4(\text{Talc}) - 356.2(\text{POE})$$
$$+ 49.8(\text{PPMA}) - 159.27(\text{Talc} \times \text{POE}) \quad (3)$$
$$- 48.37(\text{Talc} \times \text{PPMA}) - 15.16(\text{POE} \times \text{PPMA})$$
$$- 46.18(\text{Talc})^2 - 70.49(\text{POE})^2 - 8.58(\text{PPMA})^2$$

Table 4   ANOVA Analysis Data for Elastic Modulus

Source	Sum of Squares	Df	Mean Square	F value	p value	
Model	2.265×10^6	6	3.775×10^5	70.88	< 0.0001	Significant
A (Talc)	7.097×10^5	1	7.097×10^5	133.25	< 0.0001	
B (POE)	1.269×10^6	1	1.269×10^6	238.23	< 0.0001	
C (PPMA)	24,799.40	1	24,799.40	4.66	0.0563	
AB	2.029×10^5	1	2.029×10^5	38.10	0.0001	
AC	18,716.29	1	18,716.29	3.51	0.0603	
BC	1838.91	1	1838.91	0.2931	0.6051	
A^2	5712.68	1	5712.68	0.9104	0.3718	
B^2	40,071.05	1	40,071.05	7.52	0.0207	
C^2	197.04	1	197.04	0.0314	0.8644	
Residual	53,258.59	10	5325.86			
Lack-of-fit	23,068.26	8	2883.53	0.19	0.9648	Not Significant
Pure Error	30,190.33	2	15,095.17	–	–	–
Cor. Total	2.318×10^6	16	–	–	–	–
Std. Dev.	72.98		R-Squared	0.9770		
Mean	1366.87		Adj. R-Squared	0.9632		
C.V. %	5.34		Pred. R-Squared	0.9420		
PRESS	1.344×10^5		Adeq. Precision	28.717		

The high levels of factors are coded as +1 and the low levels of factors are coded as −1.

According to the p values indicated in Table 4, the effects of Talc, POE, and PPMA on elastic modulus are significant, and all insignificant terms, with p values considerably higher than 0.05, should be withdrawn from the equation. The reduced model of elastic modulus is as below:

$$E = 1424.9 + 266.4(\text{Talc}) - 356.2(\text{POE})$$
$$+ 49.8(\text{PPMA}) - 159.27(\text{Talc} \times \text{POE}) \qquad (4)$$
$$- 48.37(\text{Talc} \times \text{PPMA}) - 98.65(\text{POE})^2$$

From coefficients of Eq. (4), it can be deduced that POE has the highest impact on the elastic modulus, which is followed by Talc and PPMA. The negative coefficient indicates the downward trend of the elastic modulus with increment in the level of POE. The interaction between Talc and POE and that between Talc and PPMA are also significant, and therefore, included in the eq. A normal probability plot can be employed to determine the adequacy of the model and is applied to observe the residuals from the experimental values against the predicted values [38]. Figure 1 demonstrates the normal probability plot of the elastic modulus. Data points are close enough to the 45° line to get assured about the reliability of the derived model.

The effect of each variable on the elastic modulus is presented in Fig. 2. This type of graph is used to compare the role of various components in the design space. In these figures, one variable is changing and two other variables are fixed at their central points. By assessing the graphs, it can be found

Fig. 1 Predicted vs. Actual Values for Elastic Modulus

that increment in the percentage of Talc and PPMA leads to the enhancement of elastic modulus, but the effect of Talc is greater. However, the decrement in the elastic modulus is observed by increasing the content of the POE as an impact modifier in formulations. Based on Fig. 2, incorporation of 30% Talc and 5% PPMA caused a rise of 46% and 7.3% in the elastic modulus respectively, while adding 20% POE decreased this property by 42.3%, from 1682.45 to 970 MPa.

The increase in the elastic modulus with the increase in the percentage of the reinforcements is reported several times as a typical effect of inorganic fillers on the polymer matrix. This behavior can be indicated as follows obtained from the hydrodynamic equation of viscosity [27]:

$$\frac{E}{E_0} = \frac{\eta}{\eta_0} = 1 + 2.5\varphi + 14\varphi^2 \qquad (5)$$

where subscript 0 means the unfilled state, and φ shows the filler percentage in a composite. At a low content of Talc, the nucleation ability of this filler, which leads to the appearance of smaller and more uniform crystals, can account for the enhancement of stiffness. However, at a higher Talc concentration, modulus augmentation is related to the instinctive stiffness of Talc ($E_{\text{Talc}} \approx 170 \ GPa$ vs. $E_{PP} \approx 1.7 \ GPa$). Besides, in injection molded parts, the orientation of the plate-like Talc particles enhances the stiffness of the material [19]. Physical properties of filler such as size, aspect ratio, filler-polymer interfacial adhesion, surface characteristics, and lack of agglomerations are all important factors, on which the mechanical properties of the composite depend. Applied stress is supposed to be conveyed from the polymeric matrix to the stiff mineral in order to observe an improvement in the stiffness of the composite [27]. Good interfacial adhesion between the matrix and the filler is a consequential factor determining the properties of composites. The incorporation of the coupling agent into the formulation enhances the compatibility and the interactions between polymer and filler and leads to a better distribution of filler particles in the polymeric matrix so that a fewer number of agglomerations, which are known as stress concentration points, can be observed [28]. Increment in the content of POE causes a nonlinear reduction in elastic modulus. The POE is a thermoplastic elastomer with an approximate Tg point around −50 °C [13], and its inherent Young's modulus is much lower than that of PP. Consequently, under tensile load, the large deformation will be initially found in the POE dispersed droplets, and the stress will be mostly tackled by the PP continue phase [16]. From another perspective, the octene segments from POE structure, which have good compatibility with PP macromolecules, could curb accessibility of PP chains to spherulites resulting in less crystallinity [13]. Furthermore, poor interfacial interaction between matrix and dispersed elastomeric phase has been reported in the literature as a reason for this phenomenon [12].
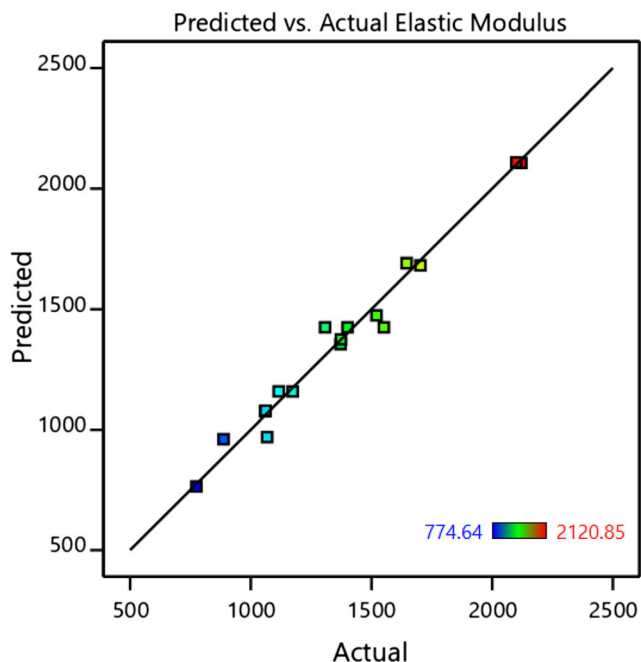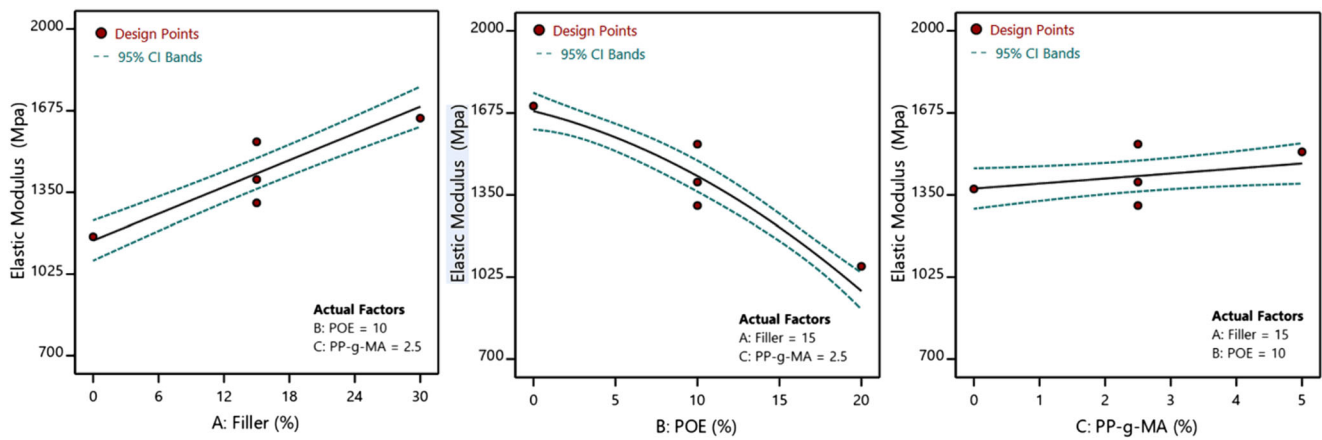
Fig. 2 One Factor Effect Plot for Elastic Modulus

The 3D surface plot and contour figure of the elastic modulus are presented in Fig. 3. The 3D surface plot is the projection of the impact of each parameter and their interactions on the responses at the same time. The percentages of Talc and POE are changing according to the horizontal axes, and the third parameter (PPMA) is kept constant at its central point. Meanwhile, the vertical axe belongs to the responses in 3D surface plots. The 3D plots can also be presented for other significant interactions. As can be seen in Fig. 3, at a higher level of POE, the effect of Talc on the increment of elastic modulus is not proportional to its content.

Tensile strength

The ANOVA analysis of the quadratic model for tensile strength is presented in Table 5. As seen in the table, p value of the model is less than 0.05 indicating that significance of

the model. The lack-of-fit is not significant evincing that the model is reliable.

The predictive model of the tensile strength (TS), which is in the form of coded factors, is submitted in the form of Eq. (6). According to the p values in Table 5, the effects of Talc, POE and PPMA on TS are significant, and all unimportant terms have been withdrawn.

$$TS = 18.42 - 0.85(Talc) - 3.14(POE)$$
$$+ 0.72(PPMA) - 0.355(POE \times PPMA) \qquad (6)$$

The tensile strength is predominantly affected by the POE content having an adverse effect. The incorporation of Talc and POE results in a lower tensile strength, while the presence of PPMA leads to an improvement. According to the p values, no significant interaction between variables is observed. Figure 4 illustrates the normal probability plot of the tensile
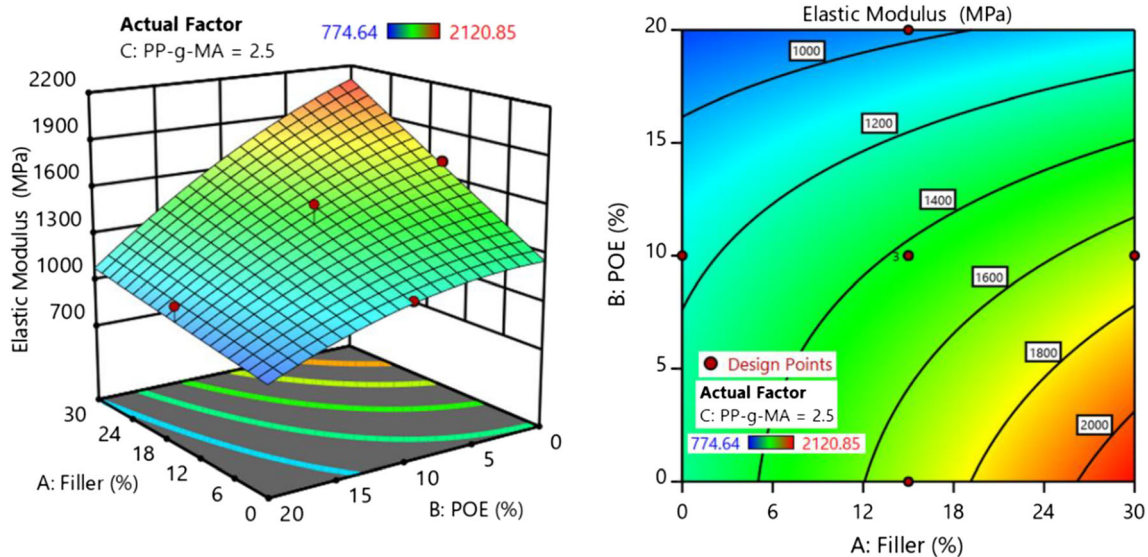

Fig. 3 3D Surface and Contour Plot of Elastic Modulus vs. Talc and POE (PPMA = 2.5%)

Table 5 ANOVA Analysis Data for Tensile Strength

Source	Sum of Squares	Df	Mean Square	F Value	p value	
Model	110.89	3	36.96	124.81	< 0.0001	significant
A (Talc)	7.24	1	7.24	24.45	0.0003	
B (POE)	98.53	1	98.53	332.72	< 0.0001	
C (PPMA)	5.11	1	5.11	17.26	0.0011	
AB	0.3042	1	0.3042	1.73	0.2293	
AC	0.3785	1	0.3785	2.16	0.1853	
BC	1.01	1	1.01	4.26	0.0614	
A^2	0.063	1	0.063	0.3591	0.5679	
B^2	0.6258	1	0.6258	3.57	0.1008	
C^2	0.2687	1	0.2687	1.53	0.2557	
Residual	3.85	13	0.30			
Lack of Fit	3.53	11	0.32	2.02	0.3778	Not Significant
Pure Error	0.32	2	0.16			
Cor Total	114.74	16				
Std. Dev.	0.54		R-Squared	0.9664		–
Mean	18.42		Adj R-Squared	0.9587		
C.V. %	2.95		Pred R-Squared	0.9339		
PRESS	7.59		Adeq Precision	35.648		

strength. As can be seen, in all design points the differences between actual and predicted values are inconsiderable verifying the acceptability of the model.

In Fig. 5, the impact of each parameter on the tensile strength is depicted. In this figure, one variable changes, and two other variables kept fixed at their central points. In fact Fig. 5 highlights the downward trend of the tensile strength for an increasing percentage of Talc and POE, even though the usage of a coupling agent has a positive implication on the improvement of this response. As can be seen from Fig. 5, adding 30% Talc reduces the tensile strength from 19.27 to 17.56 MPa, also the inclusion of 20% POE results in a drop of 29% in tensile strength. However, incorporation of 5% PPMA increases the tensile strength marginally to 19.13 MPa.

Due to poor compatibility between the matrix and filler, which are non-polar and polar, respectively, an increase in the concentration of Talc boosts the probability of filler agglomeration, particularly, at higher content of filler, and results in a reduction in the efficiency of stress transfer from matrix to reinforcement. The tensile strength is a good indicator for the status of the interfacial interactions in polymer-filler systems, and the decrement in the tensile strength exhibits inappropriate interfacial bonds between two phases [2]. A higher tensile strength represents better compatibility, and a decent compatibility leads to a higher tensile strength [19]. PPMA resin has a great impact on the interactions of Talc particles and PP segments, and it improves tensile strength by extending the interface area and by facilitating the stress conveyance from the matrix to tough particles [3]. As mentioned previously, because of its nature, POE has almost no resistance to deformations and leads to a formation of a composite with a ductile behavior, and reduction of the tensile strength through a brittle-ductile transition is inevitable a growth in POE concentration can highlight this behaviour better. Due to the lack of interactions between variables, there is no need to
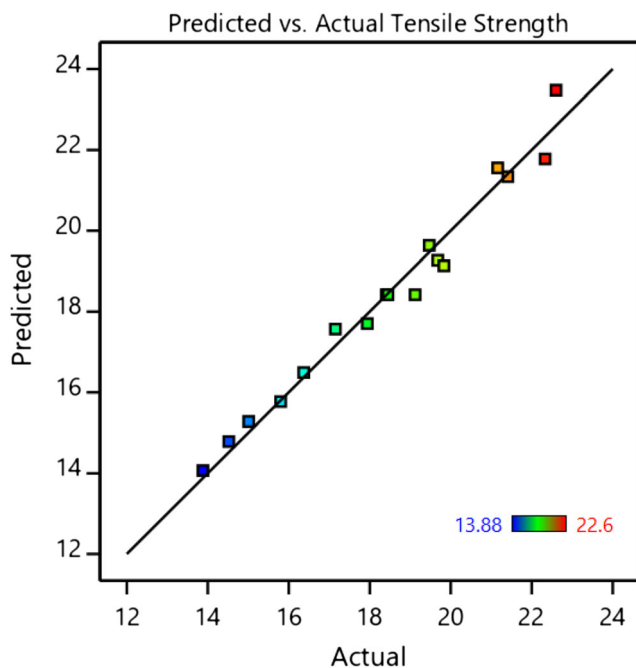
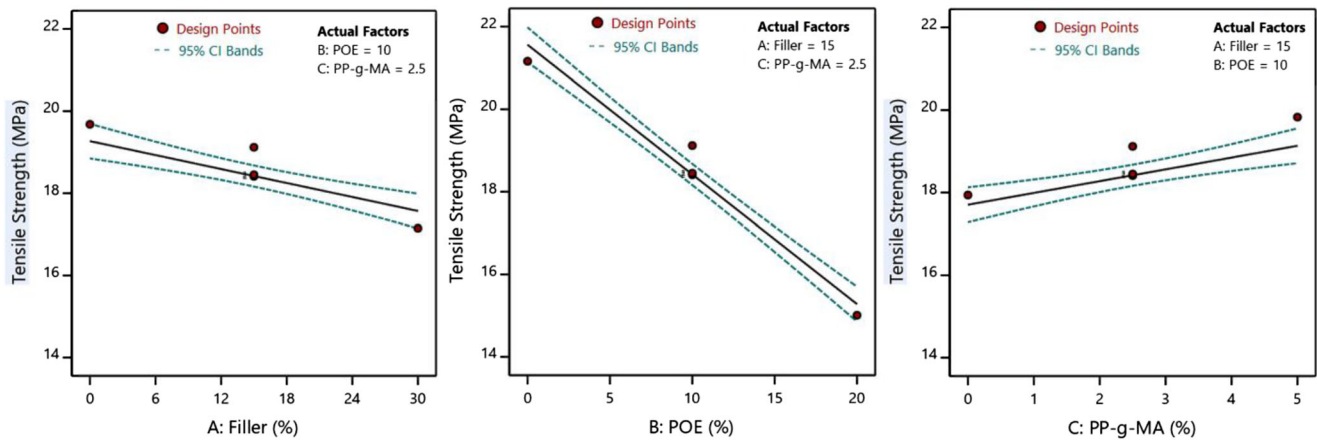**Fig. 4** Predicted Versus Actual Values for Tensile Strength

Fig. 5 One Factor Effect Plot for Tensile Strength

generate a 3D surface plot and a contour figure, as they present no useful data concerning the tensile strength.

Elongation at break

In Table 6, the ANOVA evaluation of the reduced quadratic model for elongation at break is presented. As shown, the significant model and not a significant lack of fit verify the authenticity of the fitting.

Eq. (7), which is in the form of coded factors, portrays the trend of the elongation at break (EB) in terms of variables. According to the p values given in Table 2, the impacts of Talc, POE and PPMA on the EB, and also the interaction between Talc and POE, are significant and all non-essential terms have been excluded from the eq.

$$EB = 136.19 - 64.42(\text{Talc})$$
$$+ 179.32(\text{POE}) - 27.31(\text{PPMA})$$
$$+ 29.6(\text{Talc} \times \text{POE}) + 49.89(\text{Talc})^2$$
$$+ 131.36(\text{POE})^2 \qquad (7)$$

The coefficients in Eq. (7) imply that the elongation at break is predominantly affected by the POE content bringing about enhancement in the figure of this response. With an increment in the content of Talc and PPMA in the formulation, drop in the value of elongation at break is lived up to the expectation. Figure 6 illustrates the normal probability plot of the elongation at break. The divergence between actual and predicted values is insignificant which prove the accuracy of the model.

Table 6 ANOVA Analysis Data for Elongation at Break

| Source	Sum of Squares	Df	Mean Square	F Value	p value	
Model	4.866×10^5	6	81,096.00	71.47	< 0.0001	significant
A (Talc)	41,501.94	1	41,501.94	36.58	0.0001	
B (POE)	3.215×10^5	1	3.215×10^5	283.39	< 0.0001	
C (PPMA)	7457.27	1	7457.27	6.57	0.0282	
AB	7009.87	1	7009.87	6.18	0.0322	
AC	145.1	1	145.1	0.0964	0.7652	
BC	640.64	1	640.64	0.4257	0.5349	
A^2	7539.18	1	7539.18	6.64	0.0275	
B^2	52,262.06	1	52,262.06	46.06	< 0.0001	
C^2	26.17	1	26.17	0.0174	0.8988	
Residual	11,346.15	10	1134.61			
Lack of Fit	9919.54	8	1239.94	1.74	0.4158	Not Significant
Pure Error	1426.60	2	713.30			
Cor Total	4.979×10^5	16				
Std. Dev.	33.68		R-Squared	0.9772		
Mean	242.81		Adj R-Squared	0.9635		
C.V. %	13.87		Pred R-Squared	0.9325		
PRESS	33,594.55		Adeq Precision	25.080		
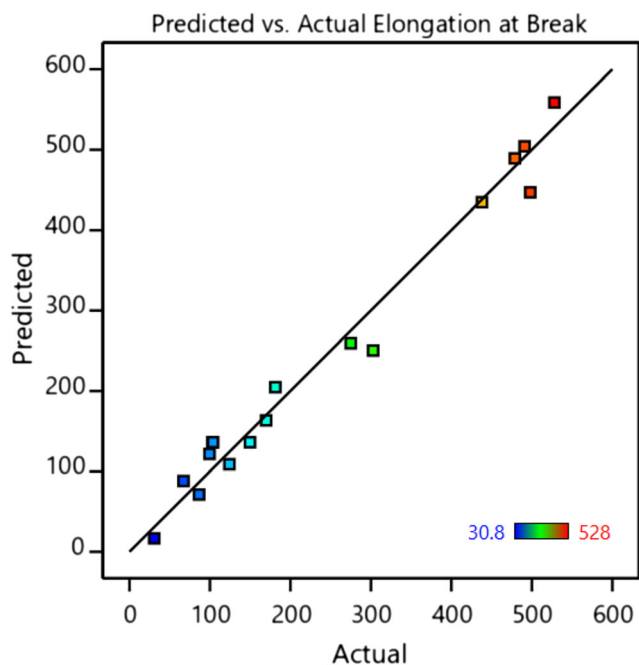
Fig. 6 Predicted Versus Actual Values for Elongation at Break

Figure 7 demonstrates the impact of each variable on the elongation at break. In these figures (Fig. 7A, B and C), one variable is changing, and the other two are kept unchanged at their central points. The graphs show that the elongation at break is decreased when the amount of Talc and PPMA are increased. However, increasing POE percentage raises the ductility of the samples. In conformity with Fig. 7, incorporation of 30% Talc and 5% PPMA decreases EB by 51.5 and 33.4% respectively. Usage of 20% POE however leads to a substantial increase in the ductility, from 88.23 to 446.8%, which shows an approximate fivefold improvement.

At a constant stress, owing to the instinctive rigidity of the filler, the inclusion of mineral filler decreases the stretching

capability of the material. Moreover, the reduction in the ductility can be associated with the stress concentration, crack initiation and propagation, which are facilitated and more conceivable at the presence of the filler [27]. When the filler is employed in the system, due to the particle–polymer interactions, the initial mobility and freedom of polymeric segments cannot be maintained so that the deformability of the matrix is restricted. As Talc is a good nucleating agent for PP, the depletion in stretching capability can be due to the alterations in morphology and crystalline structure as well [20]. At the presence of the coupling agent, the reduction in the elongation at break is intensified because PPMA can boost the particle-polymer interactions so that a fewer number of voids around the filler particles are created leading to the noteworthy reduction in the elongation at break figures. Furthermore, the improvement of interfacial interactions of two phases applies much more restraints to the freedom of polymeric chains [40]. Because of the rubbery nature of POE, an increment in the value of the elongation at break and an enhancement of deformability of the composite are expected due to its incorporation. The dispersed phase of POE demonstrates a slight resistance to the deformation and misshapes simply, and it dissipates the applied stress from tensile test leading to higher strains at the break. Also, at the presence of POE, a brittle to ductile transition likely occurs. The 3D surface plots of the elongation at break are given in Fig. 8. In each plot, the percentages of Talc and POE are changing according to the horizontal axes, and the third parameter (PPMA) is kept constant at its central point.

At the absence of POE, the decrease in the elongation at break is more prominent with the increment in the percentage of Talc. A higher amount of POE leads to a satisfactory level of ductility, regardless of the concentration of filler. The variation of the elongation at break between at a high level and at a low level of Talc at the presence of 20% POE is not significant.
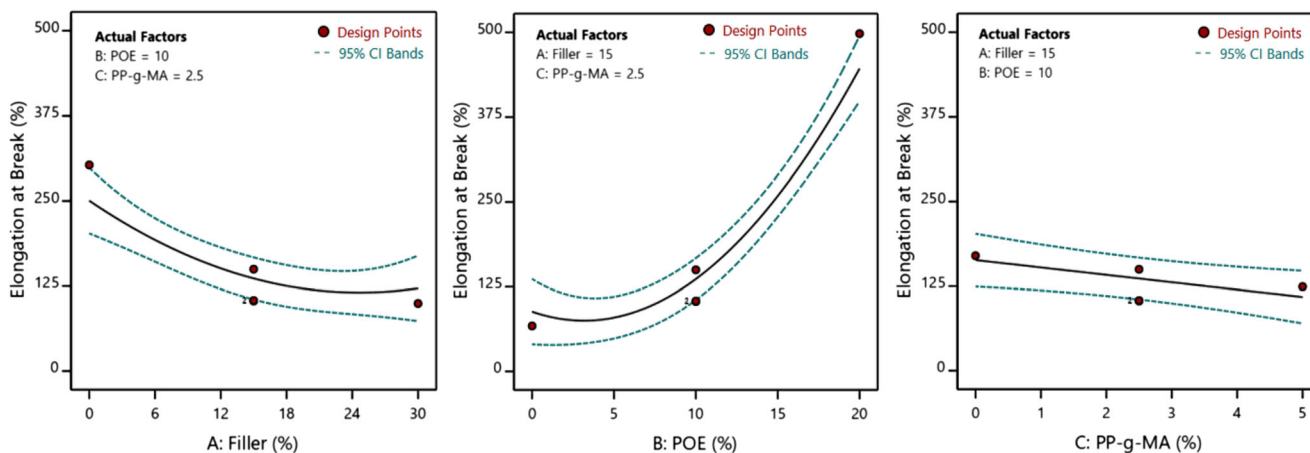

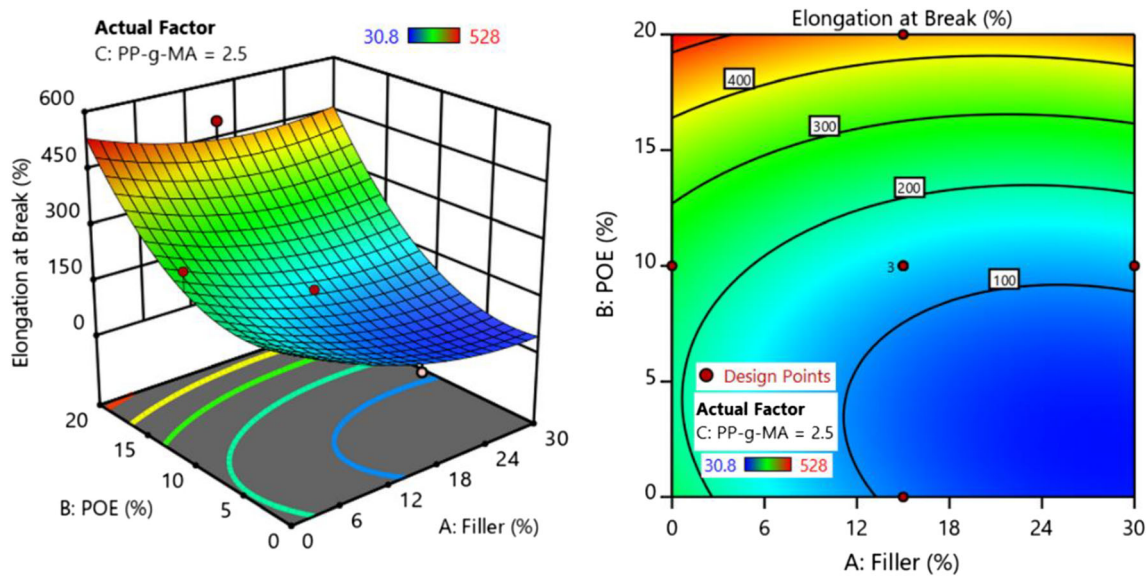**Fig. 7** One Factor Effect Plot for Elongation at Break

Fig. 8 3D Surface and Contour Plot of Elongation at Break vs. Talc and POE (PPMA = 2.5%)

Impact strength

The ANOVA analysis of the reduced quadratic model for Izod impact strength is presented in Table 7. As can be seen, the p value of the model is less than 0.05 indicating that the model is significant. The lack-of-fit is not significant proving that the model is reliable.

The predictive model of the impact strength (IS) is derived in the form of Eq. (8), in which the coded states of variables are included. According to the p values shown in Table 7, the terms Talc, POE, PPMA and the interaction of Talc/POE are significant and have an influence on IS.

$$IS = 43.81 - 5.71(\text{Talc}) + 21.26(\text{POE}) - 2.93(\text{PPMA})$$
$$+ 2.71(\text{Talc} \times \text{POE}) - 9.46(\text{POE})^2 \qquad (8)$$

It is noted from the coefficients that POE is the most influential factor among all the three individual variables, which is followed by Talc and PPMA, respectively. While the utilization of POE as an impact modifier improves the value of

Table 7 ANOVA Analysis Data for Impact Strength

| Source	Sum of Squares	Df	Mean Square	F Value	p value	
Model	5359.35	5	1071.87	93.65	< 0.0001	significant
A (Talc)	325.58	1	325.58	28.45	0.0002	
B (POE)	4520.30	1	4520.30	394.95	< 0.0001	
C (PPMA)	86.08	1	86.08	7.52	0.0191	
AB	58.92	1	58.92	5.15	0.0444	
AC	10.06	1	10.06	0.9928	0.3522	
BC	1.02	1	1.02	0.1002	0.7608	
A^2	20.33	1	20.33	2.01	0.1995	
B^2	368.46	1	368.46	32.19	0.0001	
C^2	9.22	1	9.22	0.9099	0.3719	
Residual	125.90	11	11.45			
Lack of Fit	121.61	9	13.51	6.30	0.1445	Not Significant
Pure Error	4.29	2	2.15			
Cor Total	5485.25	16				
Std. Dev.	3.38		R-Squared	0.9770		–
Mean	38.24		Adj R-Squared	0.9666		
C.V. %	8.85		Pred R-Squared	0.9476		
PRESS	287.26		Adeq Precision	29.754		
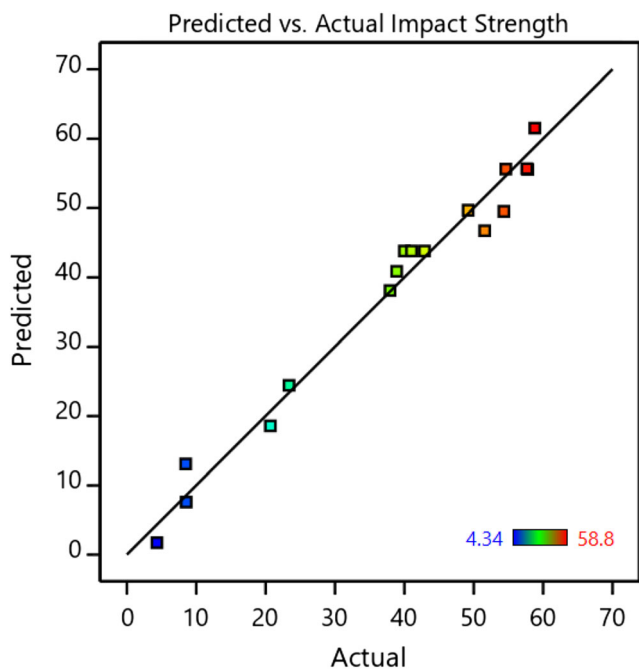
Fig. 9 Predicted Versus Actual Values for Impact Strength

impact strength, the implication of Talc as well as PPMA employment is unfavorable and results in a reduction in IS. Figure 9 illustrates the normal probability plot of IS. The experimental data well follows the diagonal line showing the adequacy of the model.

The footprints of each variable on IS are illustrated in Fig. 10, in which one variable is changing, and two others are set at their central points. The graph analyses show that despite Talc and PPMA, POE affects the impact strength positively the impact strength values of the prepared composites experienced a drop of 23% and 12.5% by incorporation of 30% Talc and 5% PPMA respectively. On the contrary, the impact strength of the sample modified with 20% POE increases significantly and reaches to 55.6 from value of 13.08 Kj/m^2.

The IS of filled polymeric composites is affected by the filler content and also the mean size of particles considerably. As the average size of the filler particles gets smaller, IS increases [27]. The interactions between polymeric chains and rigid particulates restrict the mobility of the macromolecules and make the movement and rotation more sophisticated [31]. When the filler is incorporated in the system, polymeric chains do not have enough time and mobility to deform and absorb the applied force in an impact test, which is categorized as a high-speed test [40]. Besides, at high Talc loadings, for instance, 20 $wt\%$, filler agglomerations are created with a high likelihood in reinforced composites. In comparison to the polymer-filler interactions, the filler-filler physical bonds in aggregates are too weak, resulting in the decrement in IS [21]. The incorporation of the coupling agent may put a multifaceted influence on the IS of the composite. Applying more restrictions in chains movements [40], and also rising the crystallinity fraction, PPMA would cause lower IS. From another perspective, by improving the interfacial interactions and the compatibility between the polymeric segments and filler particulates, the applied external stress can be transferred from matrix to reinforcements more straightforwardly leading to a higher resistance to a sudden fracture. During crack propagations in thermoplastic composites, the dissipation of the energy occurs with the increment in the fracture energy [21]. A shear yielding of matrix and the formation of cavitation are reported as the overriding mode of energy absorption during the impact test of elastomer toughened PP [12, 13]. A more straightforward shear yielding of the matrix implies higher impact strength of the filled composites. Big size of spherulites is considered unfavorable by hardening the shear yielding of the matrix so that stress propagation occurs with obstruction [12]. Better dispersion of filler or a smaller mean size of particulates can lead to the emergence of more sites for crystallization causing the formation of smaller spherulites that can mitigate the shear yielding of the polymeric matrix. A smaller size of the dispersed elastomeric phase is more
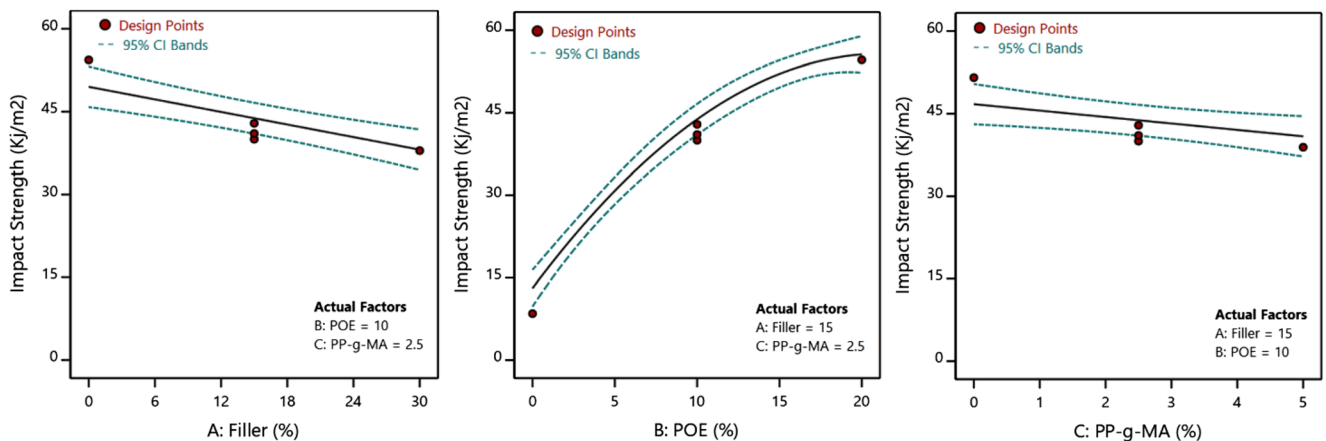

Fig. 10 One Factor Effect Plot for Impact Strength

favorable to obtain a well-toughened polymer and causes a better stress transfer through the interfaces leading to the improvement in toughness [2]. The impact strength of PP/Talc/POE ternary composites improves as the percentage of the POE increases in the formulation. Due to the coalescence of POE droplets, the efficiency of toughening is not proportional to the percentage of the employed POE and at lower contents, and the role of the POE is more noteworthy [13]. The mechanisms leading to the increment in IS in POE-toughened systems can be summarized as follows [16]: (i) a good compatibility between PP and POE leading to a well dispersion of elastomeric phase; (ii) stress concentration regions formed around POE particles under an impact load undergoing a plastic deformation and absorbing impact energy; (iii) shear yielding in the PP continuous phase around the POE particle; (iv) the prevention of further development of microcracks owing to the presence of POE particles.

The 3D surface plots of IS are presented in Fig. 11. In each plot, the percentages of Talc and POE are changing according to the horizontal axes, and the third parameter (PPMA) is kept constant at its central point.

As can be seen, in every level of Talc, decreased POE results in the decrease of IS, and this trend is more obvious at a higher amount of filler. Besides, in every level of POE, adding to filler reduces IS while this behavior is less sensitive at higher content of impact modifier.

Optimization

According to the responses defined in this experiment, the elastic modulus and tensile strength both have relations with the stiffness of the composites, while the elongation at break and IS are criteria for toughness. As a result, two groups of

mechanical properties are being affected by the content of variables conversely, which means, for example, the improvement in stiffness is at the cost of the reduction in flexibility and toughness. At this stage, our purpose is to adjust the concentration of each variable to find the optimized state by meeting the requirements for the indoor and outdoor automobile polymeric parts. According to the data obtained from a local auto manufacturer, indoor parts should have modulus, tensile strength, elongation at break and IS over 1700 MPa, 18 MPa, 25% and 15 kJ/m^2, respectively. During the optimization, each response is to be maximized under the requirements. The Desirability function (DF) method is considered as a practical method in the cases that multiple responses and diverse impacts exist. In this approach, initially, a desirability function that varies from 0 to 1 is assigned to each response. There are three types of DF available as follows, which are dependent on the nature of the issue [41]: (1) *Type 1 "the higher is better"* – this type is used for a response to be maximized; (2) *Type 2 "the lower is better"* – this type is used for a response to be minimized; and (3) *Type 3 "the nominal is better"* – this type is used for a response with a specific value. In this study, *Type 1 "the higher is better"* is employed, which is defined as Eq. (9) [39]:

$$
\begin{cases}
d_i = \left[\dfrac{Y_i - Low_i}{High_i - Low_i}\right]^{wt_i} & Low_i < Y_i < High_i \\
d_i = 0 & Y_i \le Low_i \\
d_i = 1 & Y_i \ge High_i
\end{cases}
\tag{9}
$$

where d_i is the desirability function of each response, Y_i is the answer, Low_i and $High_i$ indicate the low and the high limit of the responses and wt_i is the weight factor [1]. The high limit can be set as the target value. If $wt_i = 1$, the desirability
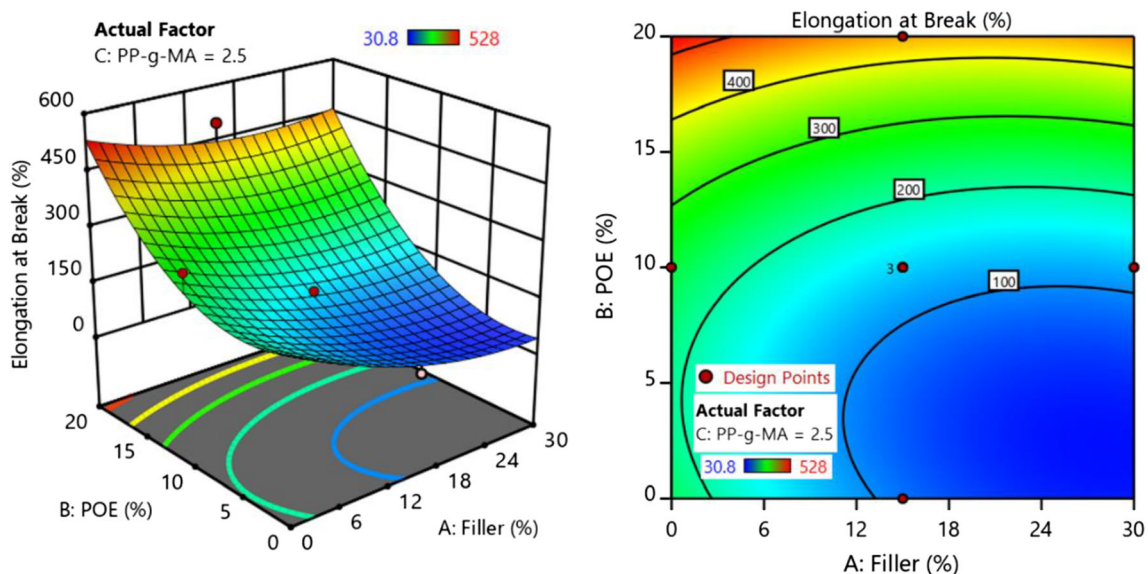

Fig. 11 3D Surface and Contour Plot of Impact Strength vs. Talc and POE (PPMA = 2.5%)

function becomes linear. By setting $wt_i > 1$, we can put pressure on the response to be closer the target value, and by setting $0 < wt_i < 1$ we can reduce the importance [42]. Considering the four responses evaluated in this study, wt_i was set to be 0.25. DF = 1 shows the ideal state. The composite desirability D(x) by uniting all desirability functions can be expressed as Eq. (10) [39]:

$$D = (d_1 \times d_2 \times \ldots \times d_n)^{\frac{1}{n}} = \left(\prod_{i=1}^{n} d_i\right)^{\frac{1}{n}} \tag{10}$$

where D is the composite desirability, n represents the number of responses and d_i is desirability function of each response. Note that all desirability functions employed in Eq. (10) have the same level of importance. Otherwise, the composite desirability should be derived in a different way. In this study, four DF according to four responses are assumed to have the same level of importance. Thus, the composite desirability in this study is derived as Eq. (11):

$$D = \sqrt[4]{d_{Modulus} \times d_{Tensile\ Strength} \times d_{Elongation\ at\ break} \times d_{Impact\ Strength}} \tag{11}$$

Design-Expert® 11 software was employed in this investigation to perform the optimization. The optimization outcomes are presented in Fig. 12. It can be seen from the figure that, to obtain an optimized condition, at which all responses and the composite desirability (D = 0.898) are maximized simultaneously, the concentration of Talc, POE and PPMA should be adjusted to 30%, 6.228% and 2.514%, respectively.

By setting the values of parameters according to the acquired optimized state, the figures of elastic modulus = 1873 *MPa*, tensile strength = 18.7 *MPa*, elongation at break = 63% and IS = 27.7 *Kj/m²* are predicted by software. Besides, it is important that as composite desirability DF = 0.898 is close to the unity, the acquired results for all responses are satisfactory. It is worth noting that if any response is entirely undesirable (d_i= 0), then DF = 0 and DF = 1 indicate a perfectly acceptable or an ideal response value for every variable. In

Table 8 Results of Confirmation Experiment According To Optimized State (Talc = 30%, POE = 6.228%, PPMA = 2.514%)

Responses	Experimental	Predicted	Deviation (%)
Elastic Modulus (*MPa*)	1842.9 ± 48	1873	1.63
Tensile Strength (*MPa*)	19.3 ± 1.9	18.7	3.1
Elongation at Break (%)	60 ± 8.4	63	5
Impact Strength (*Kj/m²*)	28.5 ± 3.2	27.7	2.8

conformity with the desirability of each response ($d_E = 0.958$, $d_{TS} = 0.784$, $d_{EB} = 0.9237$, $d_{IS} = 0.9366$), it can be concluded that the elastic modulus, IS, and elongation at break can approach their ideal value more convincing than the tensile strength. At the end of this section, a confirmation test according to the optimized state was conducted to assess the accuracy of the predicted data. The summary of results, which is a comparison between experimental and software-predicted values for responses, is presented in Table 8.

SEM micrographs

To investigate the impacts of PPMA as a coupling agent and POE as an impact modifier on morphology and mechanical properties, the SEM micrographs of the fractured surface of composites, which were obtained from Izod impact test specimens, were employed as shown in Figs. 13 and 14. To understand the role of PPMA, the SEM images of samples with 30% Talc (Figs. 13a–c) and samples with 30% talc at the presence of 5% PPMA (Figs. 13d–f) were compared at three different magnifications. In Fig. 13, the fractured surfaces are relatively smooth, depicting the brittle behavior of samples in the impact test. The presence of microvoids through fractured surfaces is due to pulled out Talc particles during the impact test. It indicates the weak interfacial interactions among filler particles and polymeric chains and implies that the applied stress cannot efficiently be transferred from the matrix to the
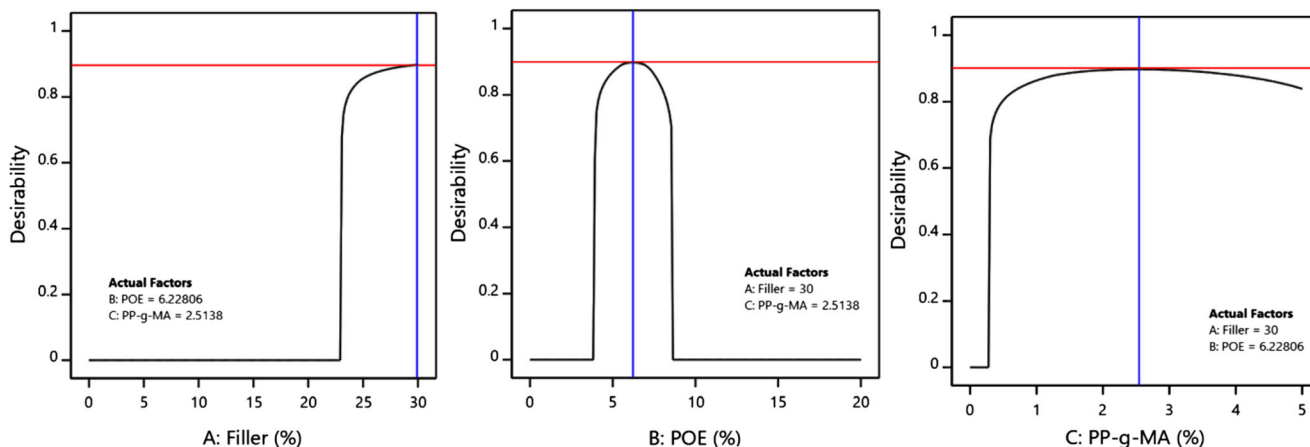
**Fig. 12** Optimization Desirability Plot against the content of variables

Fig. 13 SEM micrographs of the fractured surface of PP-based impact test specimens at various magnifications filled with: (a, b, c) 30% Talc, (d, e, f) 30% Talc+ 5% PPMA
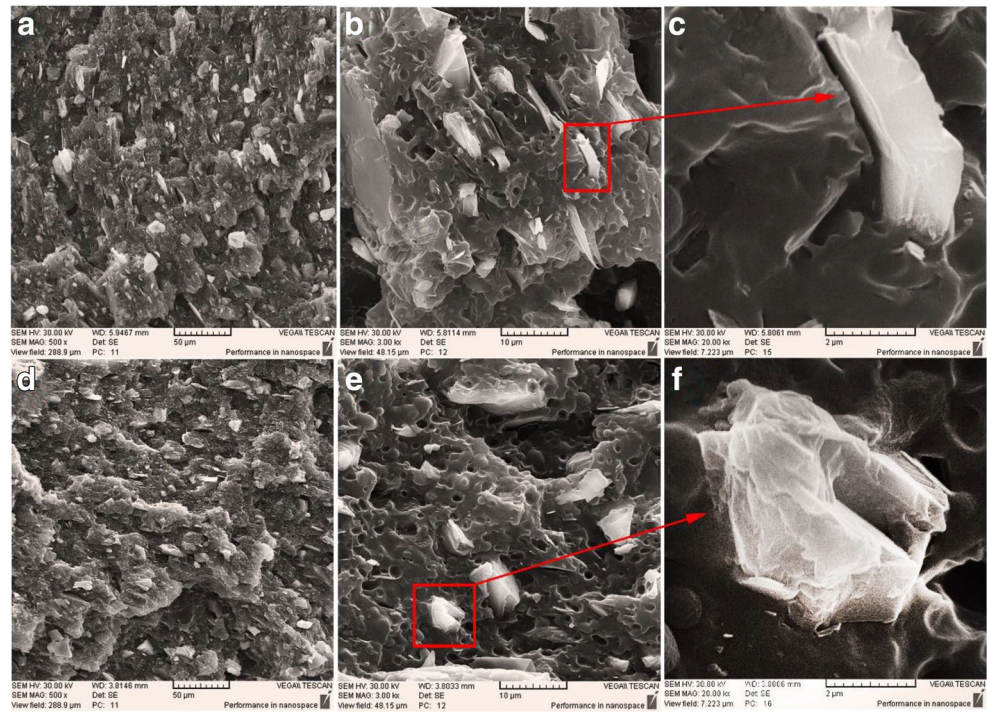
filler. An inclusion of 5% PPMA in the formulation led to a noticeable decrease in the number of microvoids (Fig. 13d). Moreover, at the presence of PPMA, more uniform dispersion of Talc particles was obtained, and the mean particle size of dispersed filler was lower, which can lead to a better stress conveyance. It can be seen in Figs. 13b and e that at the absence of PPMA, platy form Talc particulates are much more

oriented toward the injection flow and are perpendicular to the fractured surface, which can be ascribed to a fewer number of interactions among polymeric segments and tough particles. At higher magnification (Figs. 13c and f), the role of PPMA in the compatibility of two phases can be observed prominently. Residues of the matrix on the Talc surface, no clear-cut and blurred border between the two phases, and less vacant or

Fig. 14 SEM micrographs of fractured surface of PP-based impact test specimens at various magnifications etched at toluene and filled with: (a, b, c) 15% Talc+2.5% PPMA+10% POE, (d, e, f) 15% Talc+2.5% PPMA+ 20% POE
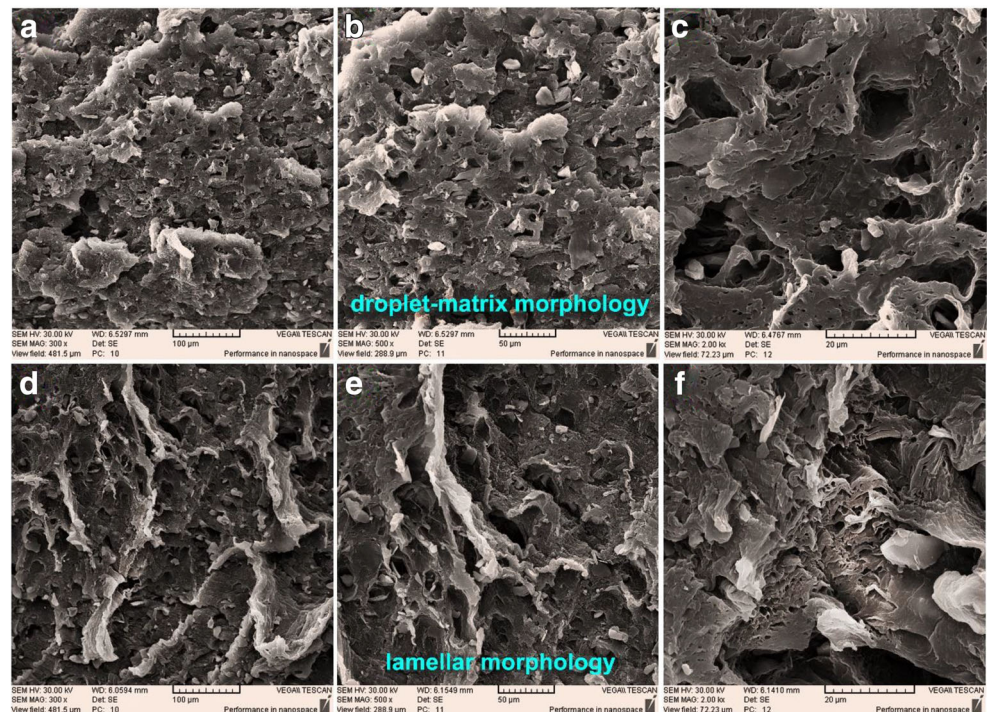
unfilled space around particulates all indicate the PPMA effectiveness. The enhancement in the mechanical properties, such as elastic modulus and tensile strength measured at a low strain, owes to better dispersion of filler in the matrix as well as better stress conveyance among phases, which are obtained due to the presence of coupling agent in the formulation.

SEM images of toluene-etched PP/Talc/POE/PPMA samples are presented in Fig. 14. The images labelled as Fig. 14a–c are linked to the samples containing 15% Talc, 10% POE and 2.5% PPMA, and images in Figs. 14d–f give information about the samples with 15% talc, 20% POE and 2.5% PPMA. In comparison to the images presented in Fig. 13, fractured surfaces at the presence of POE are rougher, showing the plastic deformation and ductile behavior of the samples. This observation is more noteworthy when the percentage of utilized POE is higher in the formulation. The vacant zones are in association with POE dispersed droplets etched by a solvent. In Fig. 14, a droplet-matrix morphology with a uniform dispersion of the elastomeric phase is observed. With an increment in POE concentration owing to the coalescence phenomena of droplets [15], the average size of POE domains as well as the shape of them altered profoundly. At a higher percentage, POE droplets became bigger with much more complex shapes and the tendency toward co-continuous and lamellar morphology. Under an impact load, the toughening effect of POE can be due to stress concentration and large deformation generated in the elastomeric phase leading to more straightforward shear yielding of PP continuous phase in proximity to POE droplets so that the applied impact energy can be dissipated better [16]. Consequently, smaller and more uniform dispersions of POE droplets in the form of droplet-matrix morphology result in higher toughening efficiency.

Thermal analysis

To investigate the impacts of Talc, POE and PPMA on the thermal properties of composites, such as melting and crystallization temperature and crystallinity content, the DSC thermograms of five samples are compared with each other in Figs. 15 and 16.

The extracted data from the melting and crystallization curves are presented in Table 9. The percentage of crystallinity is obtained using Eq. (12).

$$X_{c\,PP} = \frac{\Delta H_{m\,PP}}{(1-\omega)\Delta H_{100\%PP}} \tag{12}$$

where ω shows the weight fraction of mineral filler in the compound, $\Delta H_{m\,PP}$ is the area under the melting peak of PP in DSC thermogram and $\Delta H_{100\%\,PP}$ is equal to 209 J/g that is the standard enthalpy of PP when it is 100% crystalline [43]. As can be seen in Table 8, the melting temperature,
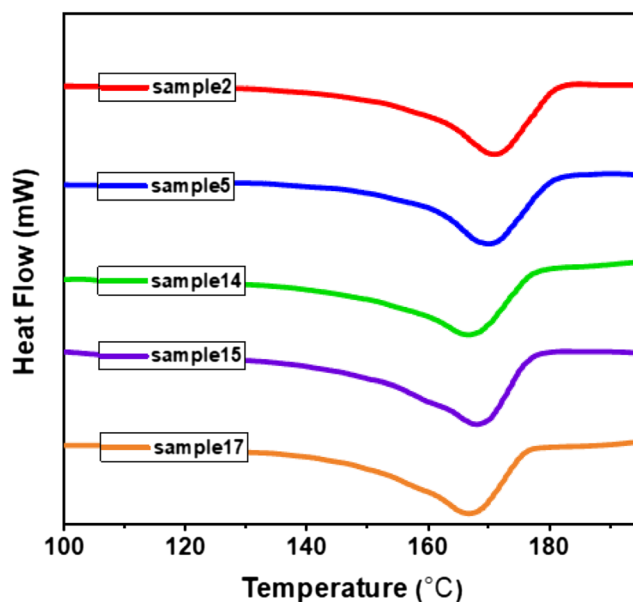

Fig. 15 Melting curves of DSC analysis

crystallization temperature and crystallinity content of virgin PP (Sample 2) are reported to be 166.6, 124.5 °C and 31.8%, respectively. The inclusion of 20% POE led to a significant drop in crystallinity to 22.5% while melting and crystallization temperature remained relatively unchanged. The reduction of crystallinity by POE utilization have been reported severally [13, 14, 16], which is due to the octene segments of POE structure that can restrain crystallization of PP segments. Thus, a decrement in the elastic modulus and improvement in the impact strength and the elongation at break of composites by incorporation of POE subsist in morphological mutations and reduction of crystallinity content to some extent. The employment of 30% Talc along with PP led to a marginal rise
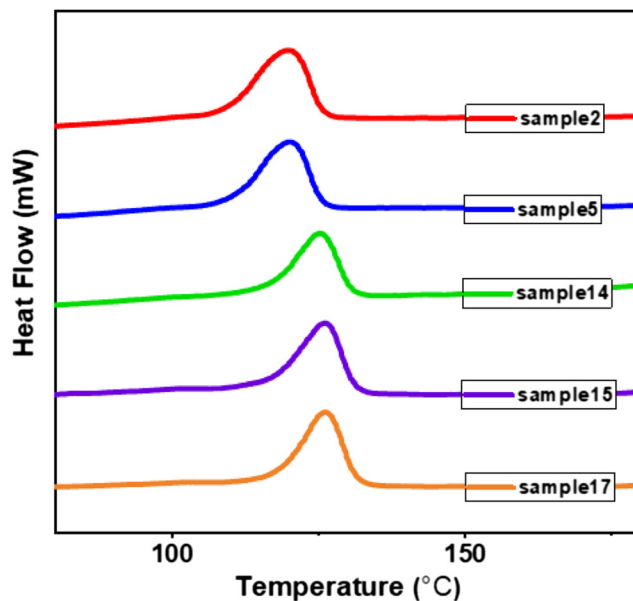

Fig. 16 Crystallization curves of DSC analysis

Table 9 Results of thermal analysis (DSC)

Sample no.	Talc%	POE%	PPMA%	ΔH_m (J/g)	T_m (°C)	$-\Delta H_c$ (J/g)	T_c (°C)	X_c (%)
2	0	0	0	66.5	166.6	87.2	124.5	31.8
5	0	20	0	47.2	165.4	67.04	124.5	22.5
15	30	0	0	47.22	164.6	53.23	130	32.3
17	30	0	5	58.25	163.8	71.54	130.9	39.8
14	30	20	5	37.12	164.2	45.4	129.8	25.3

in crystallinity content and also brought about an increase of 5.5 °C in crystallization temperature. This behavior is because of the nucleating effect of talc particulates. However, the presence of filler in the system can decrease freedom of polymeric chains so that they can reach spherulites with difficulty. Compared to virgin PP, a slight decrease in melting temperature of the Talc-filled system can be a good tribute to this impact of filler particles and indicates less packed crystals due to restrictions. An adoption of PPMA leads to better distribution and dispersion of talc particles, which is observed in SEM images as well so that more sites are available for nucleation of polymeric chains. The increment in crystallinity and crystallization temperature of a Talc-filled system at the presence of coupling agent (sample 17) and the reduction of melting temperature are all due to the more uniform dispersion of filler and better compatibility of the two phases, respectively. To sum up, the improvement of the elastic modulus by using Talc and coupling agent and the decrease in elongation at break and impact strength, which were observed in Section 3.1, can be related to the increase in crystallinity at the presence of these variables, although these materials can diminish crystallinity under a different circumstance because of polymer-filler interactions. At the simultaneous presence of Talc, POE and PPMA (Sample 14), due to contradictory impacts of materials on morphology, an intermediate state resulted.

Conclusions

In this statistical study with and optimization outlook, Response Surface Methodology with the Central Composite Design was employed to assess the properties and role of parameters in PP/Talc/POE/PPMA composite, which are commonly used in the auto industry. According to the ANOVA analysis, it was pinpointed that the incorporation of Talc in the formulation led to the improvement in elastic modulus and resulted in the decrement in the tensile strength, the elongation at break and the impact strength of the composite. By compatibilizing two phases and omitting agglomerates for more uniform dispersion of filler particulates and more efficient stress conveyance, the utilization of PPMA resulted in the enhancement in the stiffness and diminished the figures of impact strength and ductility. The improvement in the

toughness and impact energy dissipation of the composite was related to the content of the POE but at the cost of stiffness. At a high level of POE, due to morphological changes, the toughening efficiency was reduced. To optimize the content of variables and to maximize the value of responses, the desirability function method was employed. It was deduced that by incorporating 30% Talc, 6.228% POE and 2.514% PPMA in the formulation, all responses were at their apex simultaneously, with the composite desirability equal to 0.899. In the optimized state, all responses owned a higher value than what was specified in the test plan of auto indoor parts. The accuracy of the predicted data was confirmed in comparison with the experimental values. Diverse impacts of POE compared to Talc and PPMA on mechanical properties could be attributed to different morphological footprints to some extent. Compatibility of POE with PP segments resulted in lower crystallinity content, while utilization of Talc and PPMA increased the fraction of crystals.

References

1. Ashenai Ghasemi F, Ghasemi I, Menbari S et al (2016) Optimization of mechanical properties of polypropylene/talc/graphene composites using response surface methodology. Polym Test 53:283–292. https://doi.org/10.1016/J.POLYMERTESTING.2016.06.012
2. Bagheri-Kazemabad S, Fox D, Chen Y et al (2012) Morphology, rheology and mechanical properties of polypropylene/ethylene–octene copolymer/clay nanocomposites: effects of the compatibilizer. Compos Sci Technol 72:1697–1704. https://doi.org/10.1016/J.COMPSCITECH.2012.06.007
3. Jahani Y (2010) Dynamic rheology, mechanical performance, shrinkage, and morphology of chemically coupled talc-filled polypropylene. J Vinyl Addit Technol 16:70–77. https://doi.org/10.1002/vnl.20209
4. Ajorloo M, Fasihi M, Ohshima M, Taki K (2019) How are the thermal properties of polypropylene/graphene nanoplatelet composites affected by polymer chain configuration and size of nanofiller? Mater Des 181:108068. https://doi.org/10.1016/j.matdes.2019.108068
5. Tarashi S, Nazockdast H, Javidi Z, Mehranpour M (2019) Long-chain branch-induced interfacial interaction and its effect on morphology development in polypropylene/ethylene octene copolymer blend. J Mater Sci 54:6742–6751. https://doi.org/10.1007/s10853-019-03341-x
6. Mahendra IP, Wirjosentono B, Tamrin et al (2019) The influence of maleic anhydride-grafted polymers as compatibilizer on the

properties of polypropylene and cyclic natural rubber blends. J Polym Res 26:26–10. https://doi.org/10.1007/s10965-019-1878-2

7. Ghasemi FA, Niyaraki MN, Ghasemi I, Daneshpayeh S (2019) Predicting the tensile strength and elongation at break of PP/graphene/glass fiber/EPDM nanocomposites using response surface methodology. Mech Adv Mater Struct. https://doi.org/10.1080/15376494.2019.1614702

8. Fasihi M, Mansouri H (2016) Effect of rubber interparticle distance distribution on toughening behavior of thermoplastic polyolefin elastomer toughened polypropylene. J Appl Polym Sci:133. https://doi.org/10.1002/app.44068

9. Wang J, Guo J, Li C, Yang S, Wu H, Guo S (2014) Crystallization kinetics behavior, molecular interaction, and impact-induced morphological evolution of polypropylene/poly(ethylene-co-octene) blends: insight into toughening mechanism. J Polym Res 21:618–613. https://doi.org/10.1007/s10965-014-0618-x

10. Poothanari MA, Xavier P, Bose S et al (2019) Compatibilising action of multiwalled carbon nanotubes in polycarbonate/polypropylene (PC/PP) blends: phase morphology, viscoelastic phase separation, rheology and percolation. J Polym Res 26. https://doi.org/10.1007/s10965-019-1833-2

11. Wu J-H, Chen C-W, Wu Y-T et al (2015) Mechanical properties, morphology, and crystallization behavior of polypropylene/elastomer/talc composites. Polym Compos 36:69–77. https://doi.org/10.1002/pc.22914

12. Bai H, Wang Y, Song B, Han L (2008) Synergistic toughening effects of nucleating agent and ethylene–octene copolymer on polypropylene. J Appl Polym Sci 108:3270–3280. https://doi.org/10.1002/app.27980

13. Tang W, Tang J, Yuan H, Jin R (2011) Crystallization behavior and mechanical properties of polypropylene random copolymer/poly(-ethylene-octene) blends. J Appl Polym Sci 122:461–468. https://doi.org/10.1002/app.34162

14. Liu G, Qiu G (2013) Study on the mechanical and morphological properties of toughened polypropylene blends for automobile bumpers. Polym Bull 70:849–857. https://doi.org/10.1007/s00289-012-0880-1

15. Zhu L, Xu X, Ye N et al (2009) Influence of composition and phase morphology on rheological properties of polypropylene/poly(ethylene-co-octene) blends. Polym Compos 31:105–113. https://doi.org/10.1002/pc.20773

16. Liang J-Z (2012) Mechanical properties and morphology of polypropylene/poly(ethylene-co-octene) blends. J Polym Environ 20:872–878. https://doi.org/10.1007/s10924-012-0441-6

17. Hu X, Geng C, Yang G et al (2015) Synergetic effects of a matrix crystalline structure and chain mobility on the low temperature toughness of polypropylene/ethylene–octene copolymer blends. RSC Adv 5:54488–54496. https://doi.org/10.1039/C5RA09685E

18. Liu Y, Kontopoulou M (2006) The structure and physical properties of polypropylene and thermoplastic olefin nanocomposites containing nanosilica. Polymer (Guildf) 47:7731–7739. https://doi.org/10.1016/J.POLYMER.2006.09.014

19. Castillo LA, Barbosa SE, Capiati NJ (2013) Influence of talc morphology on the mechanical properties of talc filled polypropylene. J Polym Res 20:152–159. https://doi.org/10.1007/s10965-013-0152-2

20. Lapcik L, Jindrova P, Lapcikova B et al (2008) Effect of the talc filler content on the mechanical properties of polypropylene composites. J Appl Polym Sci 110:2742–2747. https://doi.org/10.1002/app.28797

21. Wang T, Liu D, Keddie JL (2007) An alternative approach to the modification of talc for the fabrication of polypropylene/talc composites. J Appl Polym Sci 106:386–393. https://doi.org/10.1002/app.26462

22. Nevalainen K, Auvinen S, Orell O et al (2013) Characterization of melt-compounded and masterbatch-diluted polypropylene composites filled with several fillers. Polym Compos 34:554–569. https://doi.org/10.1002/pc.22454

23. Sheril RV, Mariatti M, Samayamutthirian P (2014) Single and hybrid mineral fillers (talc/silica and talc/calcium carbonate)-filled polypropylene composites: effects of filler loading and ratios. J Vinyl Addit Technol 20:160–167. https://doi.org/10.1002/vnl.21347

24. Igarza E, Pardo SG, Abad MJ et al (2014) Structure–fracture properties relationship for polypropylene reinforced with fly ash with and without maleic anhydride functionalized isotactic polypropylene as coupling agent. Mater Des 55:85–92. https://doi.org/10.1016/J.MATDES.2013.09.055

25. Bouaziz A, Jaziri M, Dalmas F, Massardier V (2014) Nanocomposites of silica reinforced polypropylene: correlation between morphology and properties. Polym Eng Sci 54:2187–2196. https://doi.org/10.1002/pen.23768

26. Doufnoune R, Chebira F, Haddaoui N (2003) Effect of TITANATE coupling agent on the mechanical properties of calcium carbonate filled polypropylene. Int J Polym Mater 52:967–984. https://doi.org/10.1080/714975875

27. El-Midany AA, Ibrahim SS (2010) The effect of mineral surface nature on the mechanical properties of mineral-filled polypropylene composites. Polym Bull 64:387–399. https://doi.org/10.1007/s00289-009-0209-x

28. Mehrjerdi AK, Mengistu BA, Åkesson D, Skrifvars M (2014) Effects of a titanate coupling agent on the mechanical and thermo-physical properties of talc-reinforced polyethylene compounds. J Appl Polym Sci 131:n/a-n/a. https://doi.org/10.1002/app.40449

29. Castillo LA, Barbosa SE, Capiati NJ (2012) Influence of talc genesis and particle surface on the crystallization kinetics of polypropylene/talc composites. J Appl Polym Sci 126:1763–1772. https://doi.org/10.1002/app.36846

30. Pivsa-Art W, Fujii K, Nomura K et al (2016) Isothermal crystallization kinetics of talc-filled poly(lactic acid) and poly(butylene succinate) blends. J Polym Res 23. https://doi.org/10.1007/s10965-016-1045-y

31. Duan J, Dou Q (2013) Investigation on β-polypropylene/PP- g -MAH/surface treated talc composites. J Appl Polym Sci 130:206–221. https://doi.org/10.1002/app.39178

32. García-Martínez JM, Areso S, Taranco J, Collar EP (2009) Dynamic mechanical analysis of the interfacial changes in polypropylene/talc composites induced by different interfacial modifications from the reinforcement side. J Appl Polym Sci 114:551–561. https://doi.org/10.1002/app.30499

33. Othman NAF, Selambakkannu S, Ting TM et al (2019) Integration of phosphoric acid onto radiation grafted poly (2,3-epoxypropyl methacrylate) -PP/PE non-woven fabrics aimed copper adsorbent via response surface method. J Polym Res 26. https://doi.org/10.1007/s10965-019-1963-6

34. Ghasemi I, Karrabi M, Mohammadi M, Azizi H (2010) Evaluating the effect of processing conditions and organoclay content on the properties of styrene-butadiene rubber/organoclay nanocomposites by response surface methodology. Express Polym Lett 4:62–70. https://doi.org/10.3144/expresspolymlett.2010.11

35. Taghizadegan S (2006) Six sigma master Black Belt level case study. Essentials Lean Six Sigma:205–223. https://doi.org/10.1016/B978-012370502-0/50012-6

36. Yaghoobi H, Fereidoon A (2018) An experimental investigation and optimization on the impact strength of kenaf fiber biocomposite: application of response surface methodology. Polym Bull 75:3283–3309. https://doi.org/10.1007/s00289-017-2212-y

37. ANOVA Test: Definition, types, Examples - Statistics How To https://www.statisticshowto.datasciencecentral.com/probability-and-statistics/hypothesis-testing/anova/. Accessed 28 May 2019

38. Ashenai Ghasemi F, Daneshpayeh S, Ghasemi I (2017) Multi-response optimization of impact strength and elongation at break of nanocomposites based on polypropylene/polyethylene binary polymer matrix in the presence of titanium dioxide nanofiller. J Elastomers Plast 49:633–649. https://doi.org/10.1177/0095244316681834

39. Hosseinnezhad M, Shadman A, Saeb MR, Mohammadi Y (2017) A new direction in design and manufacture of co-sensitized dye solar cells: toward concurrent optimization of power conversion efficiency and durability. Opto-Electronics Rev 25:229–237. https://doi.org/10.1016/J.OPELRE.2017.06.003

40. Wong KW-Y, Truss RW (1994) Effect of flyash content and coupling agent on the mechanical properties of flyash-filled polypropylene. Compos Sci Technol 52:361–368. https://doi.org/10.1016/0266-3538(94)90170-8

41. Ataeefard M, Shadman A, Saeb MR, Mohammadi Y (2016) A hybrid mathematical model for controlling particle size, particle size distribution, and color properties of toner particles. Appl Phys A Mater Sci Process 122:726–714. https://doi.org/10.1007/s00339-016-0242-1

42. Daneshpayeh S, Ashenai Ghasemi F, Ghasemi I, Ayaz M (2016) Predicting of mechanical properties of PP/LLDPE/TiO2 nanocomposites by response surface methodology. Compos Part B Eng 84:109–120. https://doi.org/10.1016/J.COMPOSITESB.2015.08.075

43. Altay L, Atagur M, Sever K et al (2019) Synergistic effects of graphene nanoplatelets in thermally conductive synthetic graphite filled polypropylene composite. Polym Compos 40:277–287. https://doi.org/10.1002/pc.24643

Publisher's note Springer Nature remains neutral with regard to jurisdictional claims in published maps and institutional affiliations.